Interference Direction Finding for Aviation Applications of GPS

Konstantin Gromov, Dennis Akos, Sam Pullen, Per Enge, and Bradford Parkinson
Department of Aeronautics and Astronautics, Stanford University, Stanford, CA
Boris Pervan
Illinois Institute of Technology, Chicago, IL

BIOGRAPHY

Konstantin Gromov obtained a M.S. degree in Electrical Engineering in Leningrad Electrical Engineering Institute in 1992, B.S. degree in mathematics from Leningrad State University in 1991, and M.S. degree in Astronautics and Aeronautics at Stanford University in 1994. Currently he is working on his Ph.D. degree in Aeronautics and Astronautics at Stanford University under Prof. Bradford Parkinson. As an undergraduate and graduate student he has worked on variety of topics involving GPS, in particular LAAS.

Dr. Boris Pervan received a B.S. from the University of Notre Dame, M.S. from the California Institute of Technology, and a Ph.D. in from Stanford University, all in aerospace engineering. His doctoral research, which was focused on the application of Differential GPS to the high-integrity precision landing of aircraft, earned him the 1996 RTCA William E. Jackson Award. Previously, he was a systems engineer at Hughes Aircraft Company where he was involved in spacecraft mission optimization for numerous commercial and government satellite programs. Following completion of his doctoral work, he served as project leader for Local Area Augmentation System (LAAS) research and development at Stanford. Dr. Pervan is currently an Assistant Professor of Mechanical and Aerospace Engineering at the Illinois Institute of Technology in Chicago.

Dr. Dennis M. Akos completed the Ph.D. degree in Electrical Engineering at Ohio University conducting his graduate research within the Avionics Engineering Center. After completing his graduation he has served as a faculty member with Luleå Technical University, Sweden and is currently a research associate with the GPS Laboratory at Stanford University. His research interest include GPS/CDMA receiver architectures, RF design, and software radios.

Dr. Sam Pullen completed his Ph.D. in Aeronautics and Astronautics at Stanford University, where he is now the Technical Manager of Stanford's Local Area Augmentation System project. His research includes performance prediction, optimal system architectures, and integrity algorithms for both the Wide Area and Local Area Augmentation Systems.

Dr. Per Enge is an Associate Professor in the Department of Aeronautics and Astronautics at Stanford University. He received his Ph.D from University of Illinois. Prof. Enge's research currently centers around the use of GPS as a navigation sensor for aviation.

Dr. Bradford W. Parkinson is the Edward C. Wells Professor of Aeronautics and Astronautics at Stanford University. He served as the first Program Director of the Joint Program Office and was instrumental in GPS system development.

ABSTRACT

The Local Area Augmentation System (LAAS) is being developed by the US Federal Aviation Administration (FAA) to provide satellite navigation performance compliant with the stringent requirements for aircraft precision approach and landing. A primary design goal for LAAS is to insure that failures occurring in the ground or space segments be eliminated by the ground system before differential corrections are broadcast to users. One such failure is unintentional interference or intentional jamming in the GPS frequency band. To protect availability, ground personnel must also be able to locate and disable the interference source.

To serve this purpose, the LAAS Ground Facility may well include an Interference Direction Finder (IDF). The IDF can improve LAAS availability by rapidly and accurately

estimating the location of the source. IDF activities are implemented in parallel with reference receiver functions and may share components with the reference receivers and processors in existing LAAS prototypes.

This paper focuses on interference direction finding using interferometry. Given an undesired interference signal, measuring the signal propagation delay along the baseline between two antennas is used to estimate the direction of the signal. Measurements from the multiple baselines present in the LAAS Ground Facility are combined to estimate the location of the undesired signal transmitter.

The paper describes the Stanford Prototype IDF receiver design and presents experimental results that demonstrate the use of the IDF to detect nominal GPS signals and determine the source of interfering signals.

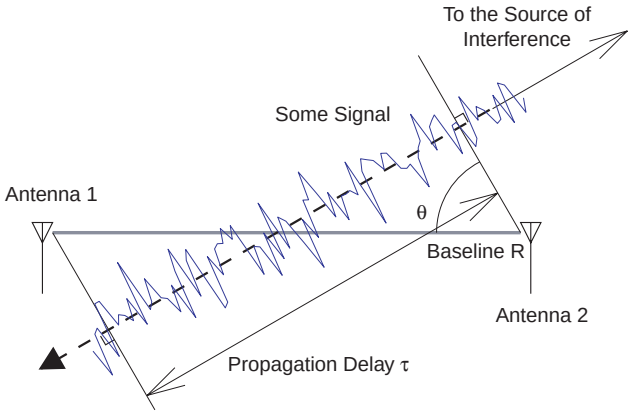

Figure 1: IDF Idea - Interferometry

INTRODUCTION

The Local Area Augmentation System (LAAS) is a ground-based differential GPS system to be implemented by the Federal Aviation Administration (FAA) for aircraft precision approach and landing. It is intended that LAAS provide Category I service for those airports that are not covered by the FAA's Wide Area Augmentation System (WAAS) and Category II and Category III performance as needed [4].

A primary design goal for LAAS is to insure that failures occurring in the ground or space segments of GPS be eliminated by the ground system before differential corrections are broadcast to users. One such failure is unintentional interference or intentional jamming in the GPS frequency band. To protect integrity, the ground and air must quickly detect the presence of interference. To protect availability, ground personnel must also be able to locate and disable the interference source. The IDF would be able to assist ground personnel in finding interference source, by providing direction and estimated location of any interfering signals that lie outside the tolerable LAAS interference environment, which is specified in Appendix H of the RTCA LAAS MASPS [5].

In order to serve this purpose, the LAAS Ground Facility may well include an Interference Direction Finder (IDF). The IDF can improve LAAS availability by accurately estimating the direction to the interference source and perhaps estimating the location of the source. IDF activities are implemented in parallel with reference receiver functions and share components with the reference receivers and processors in existing LAAS prototypes.

There are several ways to implement IDF: interferometry, time-of-arrival differential system, spatial spectrum estimation, etc. Multiple IDF algorithms can share common hardware.

Significant work has been done in the general area of estimating direction of the arrival of signals. This subject has been studied almost since invention of the radio. It is possible to classify direction finding algorithms in the following way: non-parametric algorithms: beamforming, Capon, etc., parametric methods: nonlinear least squares method, Yule-Walker method, Pisarenko and MUSIC methods, etc.

Work has also been done particularly for the GPS frequency band or for GPS related applications. It is possible to distinguish two approaches to solutions of this problem: airborne based [1] and ground based techniques [2], [3].

At Stanford University, an ongoing effort is focused on the research development, implementation, and testing of LAAS architectures and architecture subsystems. This paper considers the development of the generalized IDF receiver as part of the Stanford LAAS prototype. It can be used with a wide spectrum of direction and location-finding algorithms, such as the interferometry algorithm that is described in this paper.

IDF THEORY

As mentioned earlier there are multiple algorithms for interference direction finding. The focus of this paper is not on the direction finding algorithms per se, but on the developing universal hardware to implement and test these algorithms. This paper introduces two theoretical concepts for direction finding and location estimation using developed hardware. This is more for the illustrative purposes, how one can start using IDF hardware even without significant sophistication in algorithms.

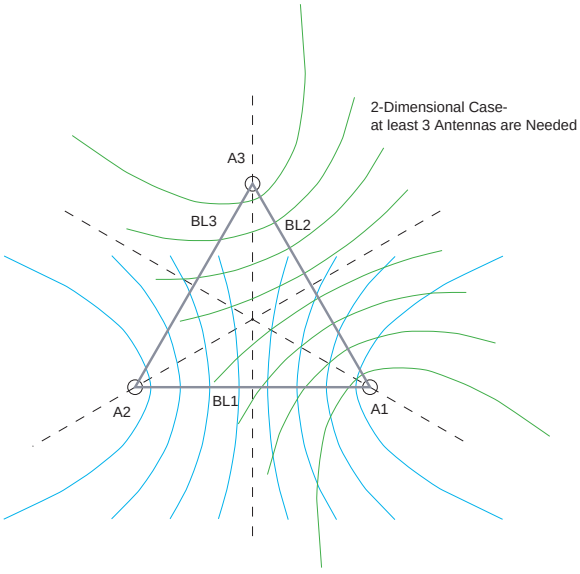

Figure 2: IDF Idea "Inverted Loran"

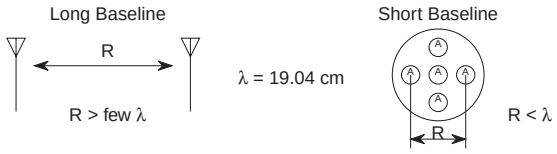

Figure 3: Long and Short Baselines

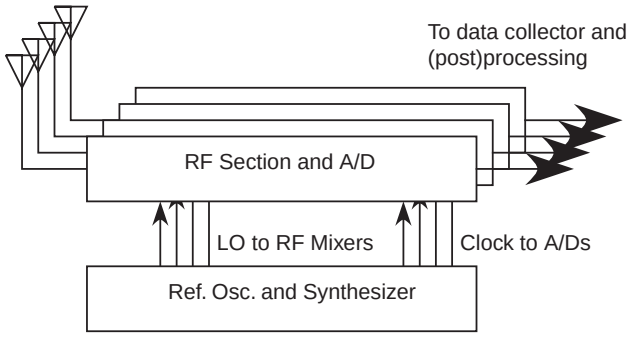

Figure 4: Diagram of IDF HW Setup

One idea, as we call it "interferometrical" approach illustrates concept and simple algorithms for the direction finding. Let's assume that source of interference is located far from the reception antenna, so we can assume planar wavefronts. Interfering signal propagating would hit Antenna 2 first and then with some propagation delay Antenna 1, as illustrated in Fig. 1. If we can somehow estimate this propagation delay τ, from the simple geometry we would be able estimate direction to the signal source. There is an ambiguity associated with the single base line, on which side of the baseline is the source, but this ambiguity could be simply resolved using multiple baselines. For many signals it is possible to estimate propagation delay τ just by correlating signals received by Antenna 1 and Antenna 2.

Another idea, which we call it "inverted Loran", also is quite simple to grasp, and it does not need an assumption about planar wavefronts. Let's look at the Fig. 2. In this case measurements are also signal propagation delay times between two antennas. For each baseline the given propagation delay would correspond to the hyperbola of possible jammer locations. Two baselines would generate two such hyperbolas. By finding their intersection we would be able estimate jammer location. There is an ambiguity in this technique, in the general case two hyperbolas could intersect in two points, but it is possible to resolve this ambiguity by various techniques, for example by adding extra baselines.

There is a way to classify antenna array by the distance between antennas relatively to the wavelength. It is easy to distinguish two cases (see Fig. 3) short baseline, when distances between antennas are smaller than a wavelength, and long baseline, when these distances significantly larger than a wavelength. IDF hardware could be used to implement various types of direction finding. To date, most our efforts have concentrated on developing IDF algorithms for the long baseline. An additional effort is underway to develop IDF algorithms for a short baseline antenna array.

Each antenna array geometry has its own advantages and disadvantages. A long baseline array is ideal to determine direction from the noise-like sources, but it would have an ambiguity for the sine-wave signal, exactly opposite is true for the short baseline antennas. Thus it would be quite useful to be able use both type of antenna arrays for IDF.

EXPERIMENTAL HARDWARE

To develop and test all possible direction finding algorithms one would need an experimental receiver. Thus a decision was made to develop 4-channel common-clock generic digital receiver, which operated in the GPS frequency band, to be used for IDF. A simplified block diagram of this receiver is shown in Fig. 4 and picture of this receiver is on Fig. 5. This receiver consists of four identical RF and A/D sections, clock section and data collector processing unit.

During the design stage of this receiver the goal was to go to the digital domain as soon as possible. So IDF receiver has only a single analog downconversion/mixing stage. The frequency plan for it is shown in Fig. 6. Signal bandwidth is kept 24 MHz until it is goes to the IF filter. There is a second downconversion, but it is done simultaneously with sampling of the signal by aliasing during A/D conversion. The frequency plan for this stage is

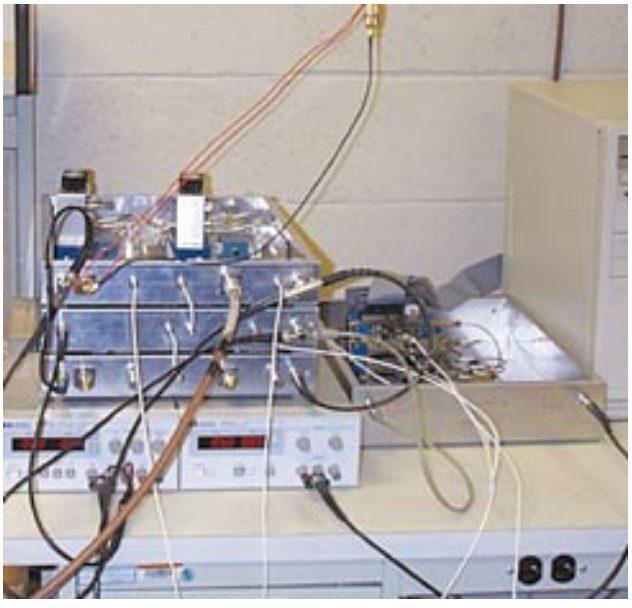

Figure 5: Picture of IDF HW Setup

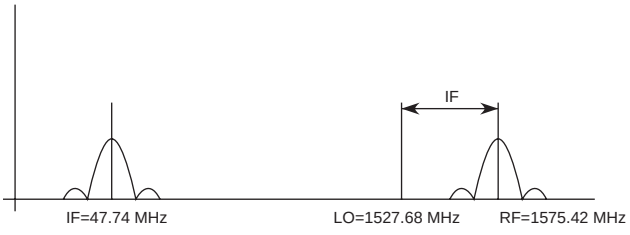

Figure 6: IDF Frequency Plan: Analog Mixing

shown on Fig. 7. Bandwidth of the IF filter was chosen to be 6 MHz, as a compromise between the resulting required digital signal processing and the bandwidth of the GPS signal, and enough bandwidth to cover main parts of the GPS band. Given sufficient digital signal processing capabilities, the IF bandwidth can be expanded to 8 MHz to satisfy the LAAS MASPS [5].

After digitization of the signal, the remainder of the processing is done completely digitally. Note that the frequency plan design has the nominal carrier frequency aliased to $f_s/4$, which would make I and Q mixing extremely simple in the digital domain, sine and cosine waves would look like series of +1, -1 and 0's.

This receiver is a full common clock architecture, thus the key elements of the system are the reference oscillator and synthesizer. The block diagram for this device is shown in Fig. 8 and picture of the real hardware in Fig. 9.

The master clock for the system is a temperature compensated crystal oscillator (TCXO) which runs at 16.368 MHz. The phase lock loop synthesizer is locked on this clock and

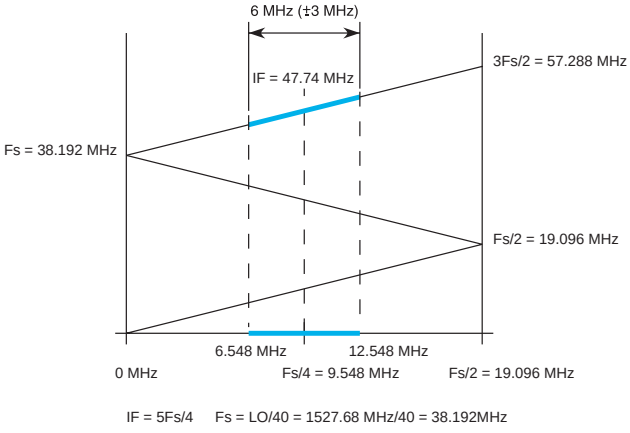

Figure 7: IDF Frequency Plan: Sampling With Aliasing

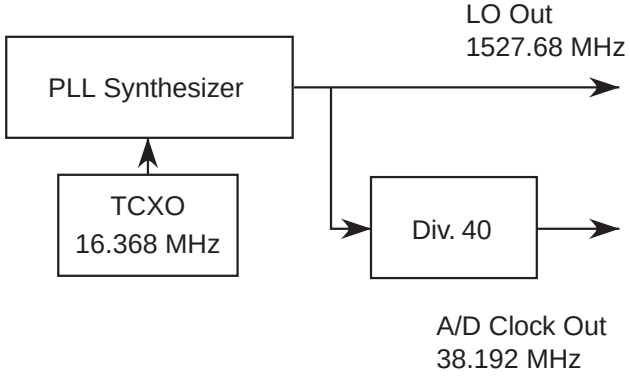

Figure 8: Common Clock Diagram

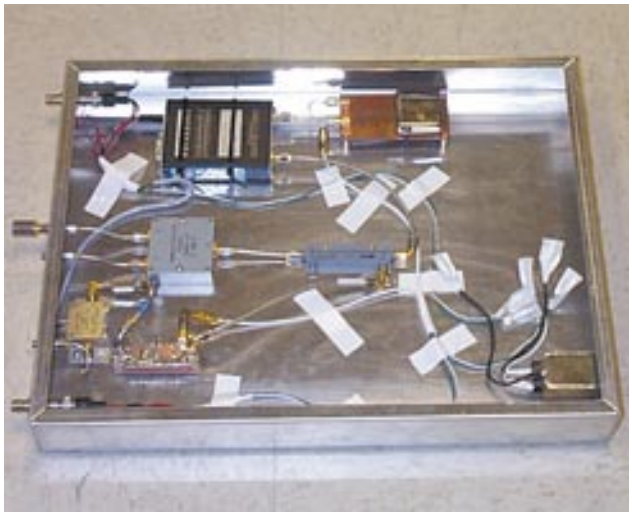

Figure 9: Common Clock Picture

Figure 10: Diagram of RF Section and A/D

Figure 11: Picture of the RF Section

generates a master frequency for the IDF receiver, which is 1527.68 MHz. This frequency is used in analog mixing of the signal, to downconvert it to the IF. This frequency also is divided by a factor of 40 by a static digital counter and then is used to drive the A/D's and strobe a digital signal into the data collector.

The combined block diagram for the RF section and A/D converter is shown in Fig. 10. There are four of these channels in the IDF receiver. The overall gain scheme assumes 25 dB gain in the antenna, and when AGC attenuator is set to the 0 (maximum gain), A/D's range would be equal to twice the variance of ambient white noise (assuming it is zero mean). (We would be able to sample ambient noise with the resolution of 12 bits.) Currently gain control is done manually, however electronically controlled attenuators are installed, and gain control software is under development.

Physically, the RF sections are combined two per chassis, and the picture in Fig. 11 shows one of these. On the front panel of the chassis, there are two antenna inputs, two IF outputs, LO input and power inputs. The system is configured such that it can supply any necessary voltage to the antenna preamplifier via RF cable.

Four A/D converters are combined together and are mounted in another chassis, as shown in Fig. 12. The IF signals go to each A/D board, and these are connected to

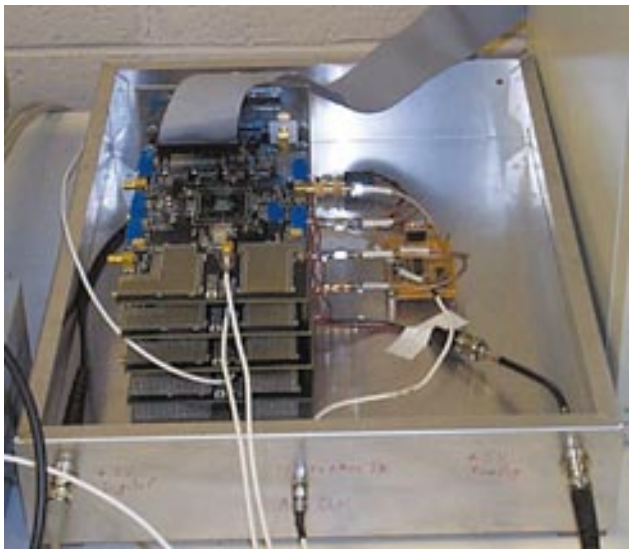

Figure 12: Picture of the A/D Module

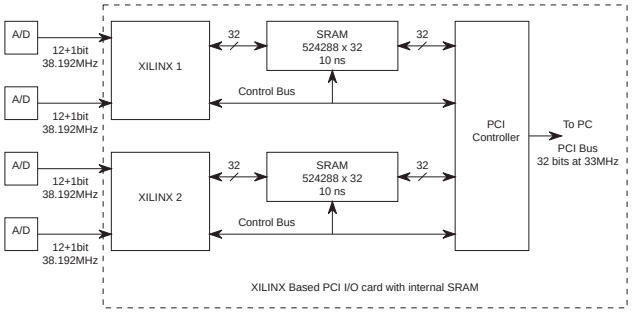

Figure 13: High Speed PCI Digital Data Collection Card

the cross board, which in turn is connected to the data collector over the ribbon cable. To accommodate the wide dynamic range of the possible signals, 12 bit converters are used. There is also an out-of-range bit on the A/D which simplifies the design of the AGC.

To collect data, we used a Xilinx based data collection and processing board with embedded SRAM. The block diagram for this board is shown on Fig. 13. There are two Xilinx FPGA chips, which are connected to the A/D data lines on one side and to the SRAM and control signals on the other side. Each FPGA is connected to the two A/D's and to the 2 MB of SRAM.

The board configuration can be easily modified by programming different code into the Xilinx chips. Eventually some of the signal processing will be done in hardware—in the FPGAs, when the algorithms would be verified and tested. Right now this board is primarily used for data collection. It is possible to configure board to store data from all four A/D's in the internal SRAM, with sequential downloading of this data into host PC. In this mode, it is possible

to collect 16.90 ms of data from 4 channels at 12 bit and out-of-range bit, sampled at 38.192 MHz. It is also possible to configure this board to collect virtually unlimited amounts of data from two A/D's utilizing DMA over the PCI bus. In this configuration, the 8 most significant bits of two A/D's are packed in 32 bit words and transfered over PCI bus into memory of the host PC. When all 4 channels are utilized it is not possible to do this as a result of limited PCI bandwidth.

SOURCE OF INTERFERENCE

Recently, much discussion has occurred regarding out-of-band emissions from handsets for the new mobile satellite communication services (MSCS). These emissions are a significant GPS interference concern. So we decided to develop a device which would imitate such emissions. Proposed specifications for out-of-band emissions from MSCS state that power levels should be no more than -70 dBW/MHz. So we created our a jammer, which is shown on the Fig. 14 such that it generates white noise across entire GPS band with a tunable power density of -70 dBW/MHz. This noise source is completely autonomously operated and is battery powered.

This interference source can be used for other experiments besides interference direction finding. When it is turned on, it does not poses a significant threat to the non-participating GPS users. Interference tests have demonstrated that it does not affect typical GPS receivers at ranges of 30 meters or more.

EXPERIMENTS

In order to confirm that the IDF equipment functions properly, we first conducted system tests in a controlled laboratory environment. These laboratory experiments were basically cable experiments. The setup for these experiments is shown in Fig. 15. The signal from the noise source is split two ways, and then each part of the signal goes into the one channel of the receiver. All cabling on one side of the split is fixed, while on the other side the cable length varies: it has been set to 3, 6, 9, and 24 feet.

Several sets of data were collected for each of the tested lengths of the second cable. Then a simple correlation algorithm was applied to the data. The resulting correlation peaks are shown in Fig. 16. Because all the signal propagation happens in the cable, it is important to take into account the speed of light in the cable to get correct differential distances. For the cable which was used, the specified value was 0.66c.

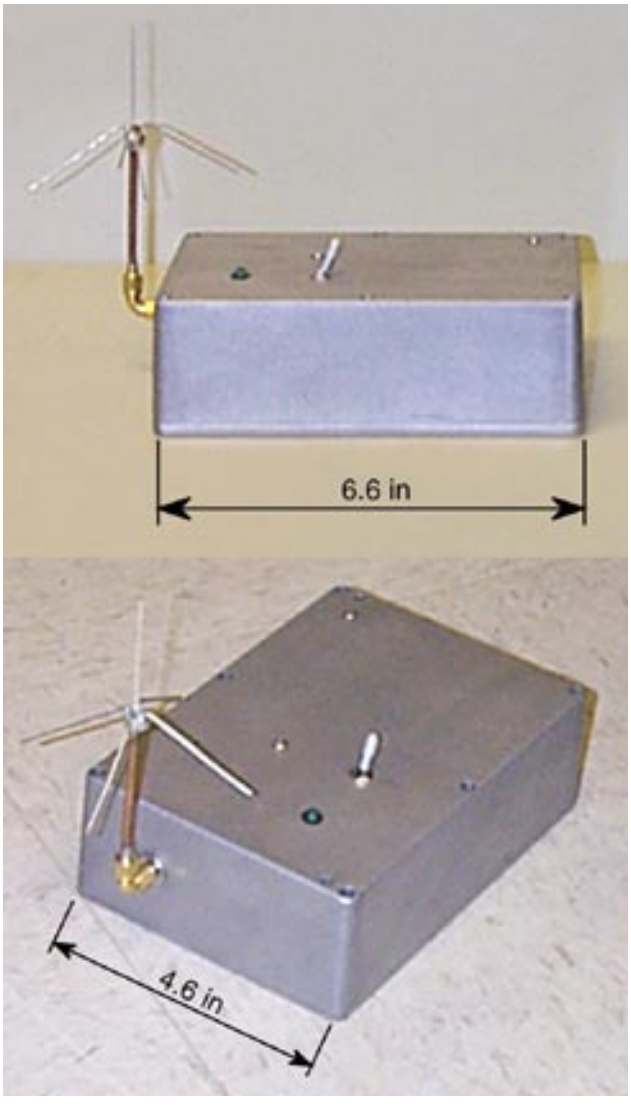

Figure 14: -70 dBW/MHz Interference Source

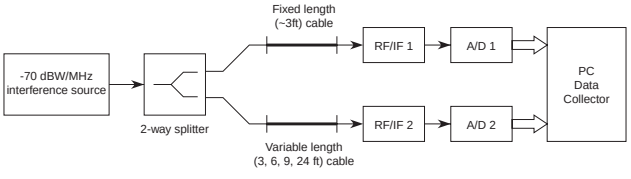

Figure 15: Cable Experiment Setup 1

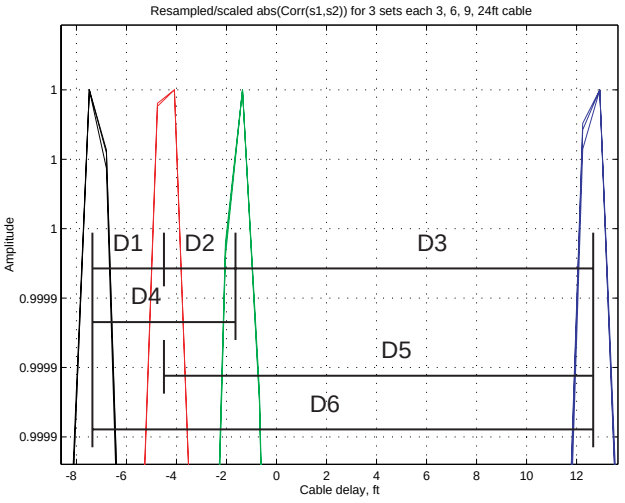

Figure 16: Cable Experiment Correlation Peaks

Cable length, ft	3ft	6ft	9ft	24ft
Measurement, ft	-7.4839	-4.0822	-1.3607	12.9268

Figure 17: Results of the Cable Experiment 1

In this cable experiment, we were looking for a good estimation of the differential length change for different cables, and were trying to estimate all system delays. So we were looking for the distances D1–D6, as shown in Fig. 16. Each of the depicted correlation peaks actually includes 3 different data collection runs, and it is easy to see that we get very good data repeatability.

In the ideal case, if cables on the both sides of the split signal path have the same length, then correlation peak should fall on 0. It was not the case in this experiment as a result of biases in the system. Fig. 17 shows the table with actual locations of the correlation peaks for each cable length. From this information it is easily to calculate differential lengths. The results of this calculation are shown in Fig. 18. Each point on the correlation peak is spaced 0.2073 m apart, or about 0.7 ft, and none of the errors exceeds 1 foot. Based on these results, we can estimate maximum of the each peak

Range	Ideal Case, ft	Measurement, ft	Error, ft
D1	3	3.4017	0.4017
D2	3	2.7215	-0.2785
D3	15	14.2875	-0.7125
D4	6	6.1232	0.1232
D5	18	17.009	-0.991
D6	21	20.4107	-0.5893

Note: 1 Sample = 0.2073 m = 0.68 ft

Figure 18: Results of the Cable Experiment 2

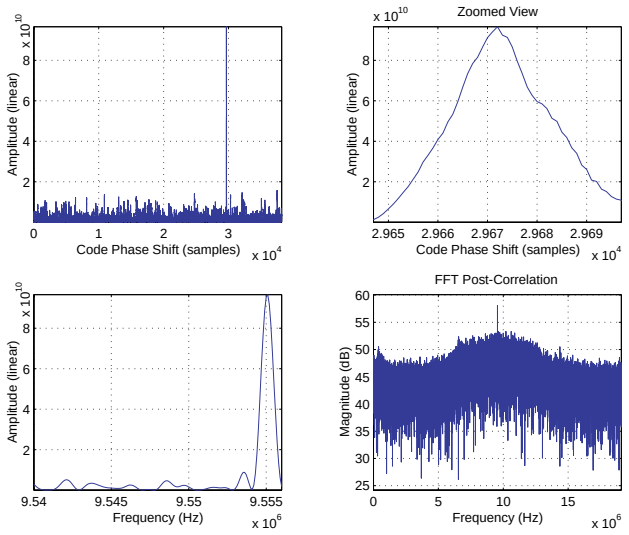

Figure 19: System Calibration Using GPS

with 0.4 ft error, and the differential error should not exceed 0.7 ft. The differential range measurement accuracy of 0.2073 m in the cable corresponds to 0.3142 m in open air because of the greater speed of light in air. This test confirms that the IDF equipment works as expected, and the biases in the system can be calibrated.

The next experiment was an open air experiment. The goal of this test was to show that this receiver is capable of acquiring real GPS signals, even from short glimpses of data, as a second means of calibrating the system. It is not a good idea to try to calibrate system by introducing signal source in the GPS band. But there are signal sources in the GPS band— GPS satellites themselves— that we can use to calibrate the IDF. To calibrate the IDF, first we have to acquire GPS signals, get broadcast data, and then do system calibration using carrier phase.

To demonstrate these capabilities, 1 ms of data has been collected and then processed by GPS acquisition code. The results of this processing are shown in Fig. 19. This figure shows acquisition of one satellite— PRN 18— but data can be recycled, and we can repeat this for any satellite. The first plot shows the code shift of PRN 18 with respect to the beginning of the collected data. It effectively is the pseudorange. When we repeat this procedure for all SVs, we get enough pseudoranges to do a position fix, assuming that we have broadcast data from the satellites. The second plot shows same correlation peak, but magnified. This shows the potential of this system to be used as a Signal Quality Monitor (SQM) for the Local Area Augmentation System (LAAS). The third plot shows the correlation peak in the frequency domain, or estimation of the Doppler shift (one has to keep in mind that processing done is at IF, which is 9.548 MHz). The last plot on this figure shows the signal

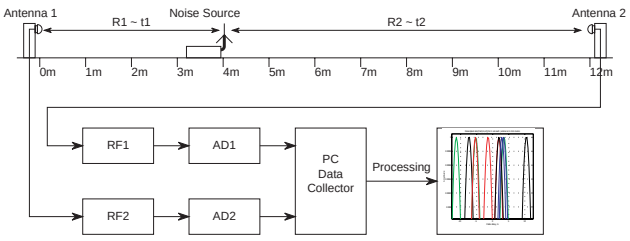

Figure 20: Rooftop Test Range 1

Figure 21: Rooftop Test Range 2

spectrum after despreading. It is easily to see the spike in the middle, which corresponds to the carrier. That restored carrier could be used to calibrate IDF receiver. This signal acquisition/calibration algorithm could be implemented on the FPGA in real time.

These experiments clearly demonstrate that it is possible to calibrate IDF hardware by utilizing the GPS signal, and it also demonstrates that it is possible to get a GPS position fix from just 1 ms of data, assuming that we have a data broadcast by satellite.

The last experiments to be discussed in this paper are experiments on the roof of the GPS lab which simulate system operation in the real environment. The system configuration for the real operation of IDF in the LAAS environment would include multiple antennas spaced a few hundreds meters apart on the airport property. Before going to the real field, we are trying to do as many experiments in the lab environment as possible. So a 12 meter test range has been settled up on the roof of the GPS lab. The length of 12 meters is defined by the roof size. The IDF system should show the capability of accurate estimation of signal time-of-arrival difference, when signal coming from any direction. It is difficult to move jammer around GPS lab in the circle, so it has been decided to move jammer on the straight line between two antennas. Effectively it is exactly the same as moving jammer around. By moving jammer between antennas we can make all possible differential times of arrival for the given antenna configuration.

The diagram for the test range is shown in Fig. 20. There are two antennas which located at the marks 0 m and 12 m, and the roving jammer which could be placed anywhere between the two antennas. We painted one meter marks between two antennas and were using them to set up a jammer in order to get repeatability in the results. To improve antenna gain in horizontal direction we mount antennas sideways toward the jammer, when in the next test we are planning to use vertically mounted dipole antennas. Signal from each antenna goes through the cable down to the lab in to the IDF receiver, where digitized, and stored in the PC computer for postprocessing. Pictures of the test range and each antenna are shown in Fig. 21.

The goal for this test is to evaluate how accurately we can measure $\tau = t_2 - t_1$, or differential range $\Delta R = c\tau$, where c is the speed of light, in the real environment, and evaluate potential problems.

Some results from this experiment are present in Fig. 22 in the form of the correlation plots for each jammer location from 1 to 11 m. In each location data has been collected 3 times length for each data set of 524288 samples, or 13.7 ms. The same results, but in tabular form are presented in Fig. 23. Results for all data runs in each location are consistent and repeatable. Error for the results at 1, 2, 3, 4, and 5 meter marks are compatible with length of one sample, which is 0.3142 m. This is is quite good results, and they demonstrate system potential. There is one outlier in the position estimation— location at 10 m mark, but this error is repeatable, from test to test, so it appears that the measurements are being affected by multipath or some other external error source. Results in other locations can be varying but multipath is the suspect. There is RF reflecting structures on the roof, which from my estimation could corrupt results on second half of the test range, but more investigation is required.

It has been demonstrated that it is possible to resolve range to 1 m in the open air tests and to 0.2074 m in the cable test. One meter error on 100 m baseline would correspond to an angular error in estimating direction of the signal of 0.6 degrees in direction perpendicular to baseline and 8 degrees along the baseline. Because of multiple baseline utilization this error could be under 1 degree for a multiple baseline system.

CONCLUSIONS

We have developed a 4-channel, common-clock high dynamic range digital receiver which operates in the L1 GPS

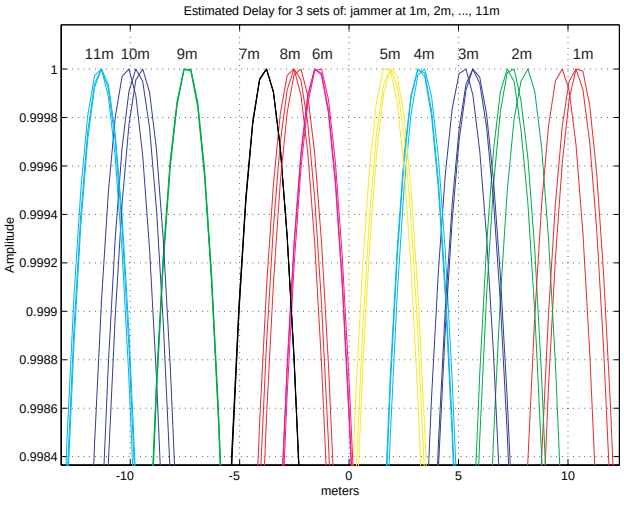

Figure 22: Plot of the Results from the Roof Experiments

Jammer location,m	Expected Delay, m	Data Set #1			Data Set #2			Data Set #3		
		Delay, Sample	Delay, m	Error, m	Delay, Sample	Delay, m	Error, m	Delay, Sample	Delay, m	Error, m
1	10	10034	10.3686	0.3686	10034	10.3686	0.3686	10032	9.7402	-0.2598
2	8	10027	8.1692	0.1692	10025	7.5408	-0.4592	10024	7.2266	-0.7734
3	6	10018	5.3414	-0.6586	10019	5.6556	-0.3444	10019	5.6556	-0.3444
4	4	10012	3.4562	-0.5438	10011	3.142	-0.858	10011	3.142	-0.858
5	2	10007	1.8852	-0.1148	10007	1.8852	-0.1148	10006	1.571	-0.429
6	0	9996	-1.571	-1.571	9996	-1.571	-1.571	9997	-1.2568	-1.2568
7	-2	9989	-3.7704	-1.7704	9989	-3.7704	-1.7704	9989	-3.7704	-1.7704
8	-4	9993	-2.5136	1.4864	9993	-2.5136	1.4864	9994	-2.1994	1.8006
9	-6	9978	-7.2266	-1.2266	9977	-7.5408	-1.5408	9977	-7.5408	-1.5408
10	-8	9969	-10.0544	-2.0544	9970	-9.7402	-1.7402	9971	-9.426	-1.426
11	-10	9965	-11.3112	-1.3112	9965	-11.3112	-1.3112	9965	-11.3112	-1.3112

Note: 1 Sample = 0.3142 m Very Good Results OK Results Bad results - Suspected multipath

Figure 23: Summary of the Results from the Roof Experiments

band. Primary intended use for this receiver is Interference Direction Finding, but it also could be used for other GPS related projects, such as SQM.

Interference tests with a 12-meter baseline show the potential to resolve differential range better than 1 m utilizing simple correlation methods. This corresponds to a timing resolution of 3.3 ns. The IDF can improve overall LAAS availability by finding direction or location of any interference sources.

ACKNOWLEDGMENTS

We would like to thank our colleagues for the help they provide to us while we are working on the project. We also would like to thank Stanford University and academic community for the nice environment to work and communicate with people. And our special thanks to the Federal Aviation Administration for the support and funding of this project.

REFERENCES

1. M. Geyer, B. Winer, R. Frazier. "Airborne GPS RFI Localization Algorithms," *Proceedings of ION GPS-97*, Kansas City, Sept. 16-19, 1997, pp. 1447-1456.

2. S.-C. Leung, R. DiEsposti, C. Giron, I. Weiss. "Analysis of Algorithms for GPS Interferer Direction Finding," *Proceedings of ION GPS-97*, Kansas City, Sept. 16-19, 1997, pp. 339-347.

3. D.-J. Moelker. "Multiple Antennas for Advanced GNSS Multipath Mitigation and Multipath Direction Finding," *Proceedings of ION GPS-97*, Kansas City, Sept. 16-19, 1997, pp. 541-550.

4. Swider, R., Recommended LAAS Architecture, Presented to RTCA SC-159, WG-4, Anaheim, CA, November 12, 1996.

5. Minimum Aviation System Performance Standards for the Local Area Augmentation System. Washington, D.C.: RTCA DO-245, September 28, 1998.